

Studies of CMB structure at Dec=+40°.

II: Analysis and cosmological interpretation

S. Hancock¹, C.M. Gutierrez², R.D. Davies³, A.N. Lasenby¹, G. Rocha¹,
R. Rebolo², R.A. Watson^{2,3} and M. Tegmark⁴

¹*Mullard Radio Astronomy Observatory, Cavendish Laboratory, Madingley Road, Cambridge CB3 0HE, UK*

²*Instituto de Astrofísica de Canarias, 38200 La Laguna, Tenerife, Spain*

³*University of Manchester, Nuffield Radio Astronomy Laboratories, Jodrell Bank, Macclesfield, Cheshire, SK11 9DL, UK*

⁴*Max-Planck-Institut für Physik, Föhringer Ring, D-80805 München, Germany*

ABSTRACT

We present a detailed analysis of the cosmic microwave background structure in the Tenerife Dec=+40° data. The effect of local atmospheric contributions on the derived fluctuation amplitude is considered, resulting in an improved separation of the intrinsic CMB signal from noise. Our analysis demonstrates the existence of common structure in independent data scans at 15 and 33 GHz. For the case of fluctuations described by a Gaussian auto-correlation function, a likelihood analysis of our combined results at 15 and 33 GHz implies an intrinsic *rms* fluctuation level of 48_{-15}^{+21} μK on a coherence scale of 4°; the equivalent analysis for a Harrison-Zel’dovich model gives a power spectrum normalisation of $Q_{rms-ps} = 22_{-6}^{+10}$ μK . The fluctuation amplitude is seen to be consistent at the 68 % confidence level with that reported for the COBE two-year data for primordial fluctuations described by a power law model with a spectral index in the range $1.0 \leq n \leq 1.6$. This limit favours the large scale CMB anisotropy being dominated by scalar fluctuations rather than tensor modes from a gravitational wave background. The large scale Tenerife and COBE results are considered in conjunction with observational results from medium scale experiments in order to place improved limits on the fluctuation spectral index; we find $n = 1.10 \pm 0.10$ assuming standard CDM with $H_0 = 50 \text{ km s}^{-1} \text{ Mpc}^{-1}$.

Key words: Cosmology - Large Scale Structure of the Universe - Cosmic Microwave Background

1 INTRODUCTION

Observations of fluctuations in the Cosmic Microwave Background (CMB) have been widely recognized to be of fundamental significance to cosmology, offering a unique insight into the physical conditions in the early Universe. The amplitudes and distribution of such fluctuations provide critical tests of the origin of the initial perturbations from which the structures seen today have formed. On scales \gtrsim few degrees, CMB observations probe scales of 1000’s of Mpc, inaccessible to conventional astronomy. At these large angles, the structures form part of an intrinsic spectrum of fluctuations generated through topological defects or inflation. In this linear growth regime, observations of the scalar CMB fluctuations provide a clean measure of the normalisation of the intrinsic fluctuation power spectrum. This normalisation has been established by a number of independent CMB observations (Smoot *et al.* 1992, Ganga *et al.* 1993,

Hancock *et al.* 1994). In many theories, tensor CMB fluctuations from a background of gravitational waves are also expected to be significant on these large scales, and measuring the slope of the power spectrum offers the potential to constrain this contribution to the CMB anisotropy (Hancock *et al.* 1994, Steinhardt 1993, Crittenden *et al.* 1993). A comparison of the large-scale anisotropy results with those on medium scales can also be used to separate the scalar and tensor components under the assumption of a specific cosmological model.

The Tenerife CMB experiments were initiated in 1984, with the installation of the first 10 GHz switched-beam radiometer system at the Teide Observatory on Tenerife Island. A subsequent programme of development has led to the present trio of independent instruments working at 10, 15 and 33 GHz. The ultimate objective is to obtain three fully sampled sky maps covering some ~ 5000 square degrees of the sky at each frequency and attaining a sensitiv-

ity of $\sim 50 \mu\text{K}$ at 10 GHz, and $\sim 20 \mu\text{K}$ in the two highest frequency channels. Drift scan observations have been conducted over a number of years covering the sky area between $\text{Dec}=+30^\circ$ and $+45^\circ$. The deepest integrations have been conducted in the $\text{Dec}=+40^\circ$ region and resulted in strong evidence for the presence of individual CMB features (Hancock *et al.* 1994).

Davies *et al.* 1995 (hereafter Paper I) described the performance of the experiments and gave an assessment of the atmospheric and foreground contributions to our data at $\text{Dec}=+40^\circ$; here we analyse in detail the results and cosmological implications of such observations. Section 2 describes the observational strategy and presents the stacked scans at each frequency. In Section 3 we use several statistical methods to calculate the level of the detected signals and their origin. A statistical comparison with the results of the COBE DMR two-year data is conducted in Section 4 and used to place limits on the spectral index of the primordial fluctuations. In Section 5 we use the additional information provided by medium-scale anisotropy results to provide improved limits on n .

2 THE SCANS AT DEC $+40^\circ$

2.1 Observations

Observations were conducted at the three frequencies 10, 15 and 33 GHz by drift scanning in right ascension at a fixed declination of 40° . The measurements were made independently at each frequency, using separate dual-beam radiometer systems as described in Paper I. The three instruments are physically scaled so as to produce approximately the same beam pattern ($\text{FWHM} \sim 5^\circ$) on the sky, thus allowing a direct comparison of structure between frequencies. A characteristic triple beam profile (switching angle $8^\circ:1$) is obtained by the combination of fast switching (63 Hz) of the horns between two independent receivers and secondary switching (0.125 Hz) provided by a wagging mirror. We make repeated observations of the sky, binning the data in 1° intervals in RA and stacking them together in order to reduce the noise as compared with individual measurements. As a consequence of using two independent channels, the receiver noise contribution to the final data scans is reduced by a factor $\sqrt{2}$ compared with single channel observations.

The data considered in this paper are the same as those presented in the preliminary report by Hancock *et al.* (1994). As before we restrict our analysis to the RA range $161^\circ - 230^\circ$ corresponding to Galactic latitude $b > 56^\circ$. At these high latitudes foreground emission from the Galaxy is expected to be at a minimum. This sky region has also been selected (see Paper I) to be free from discrete radio sources above the 1.5 Jy level at 10 GHz; assuming a flat spectrum this corresponds to an antenna temperature contribution of 48, 21 and $5 \mu\text{K}$ at 10, 15 and 33 GHz respectively in the $\text{Dec}=+40^\circ$ data. The actual contamination is reduced below these levels by using the Kühr catalogue (Kühr *et al.* 1981) supplemented by the VLA calibrators list to subtract the discrete source contribution from each data scan. This amounts to making corrections to the *rms* signal level of 13, 8, and $3 \mu\text{K}$ at 10, 15 and 33 GHz respectively. The contribution of unresolved radio sources is expected to be

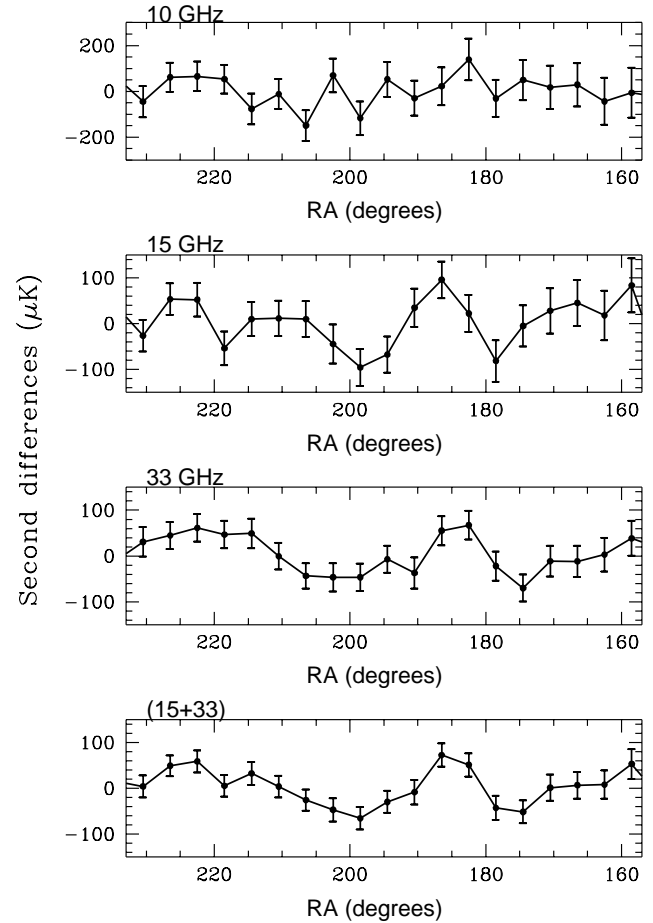


Figure 1. The stacked scans at $\text{Dec}=+40^\circ$. The second differences in temperature are shown binned at 4° intervals in RA. The error bars are at 68 % confidence and take into account any atmospheric correlations between receiver channels. The scans labeled 15+33 represent the weighted addition of the data at 15 and 33 GHz.

$\Delta T/T \leq 5 \times 10^{-6}$ at 15 GHz and significantly smaller at 33 GHz (Aizu *et al.* 1987, Franceschini *et al.* 1989).

Figure 1 presents our final stacked scans at 10, 15, 33 GHz and the weighted addition (named 15+33) of the data at the two higher frequencies. We have calculated the standard error-bars of each point considering the presence of correlated atmospheric noise between the two channels of each receiver system as described in Paper I. This represents a mean enhancement of 3 % at 10 GHz, 4 % at 15 GHz, and 16 % at 33 GHz with respect to the estimation of the noise computed in Hancock *et al.* (1994). The revised sensitivities per beam-sized area are 61, 32, 25 and $20 \mu\text{K}$ at 10, 15, 33 and 15+33 respectively. A visual inspection reveals the presence of common features in the scans at the two higher frequencies; this is supported by a cross-correlation analysis in Section 3.2.

2.2 Reliability of the detected signals

Determination of the amplitude of the CMB component of the structure requires one to consider the contributions of random noise and foreground signals to the observed data scans. The former has its origin in the thermal variations in the receivers and in the fluctuating component of the atmosphere, whilst the latter consists primarily of free-free and synchrotron emission in the Galaxy, plus emission from the Sun and Moon. Of these effects, only the Galactic emission remains constant from day to day at a given frequency. In Paper I we have estimated a maximum Galactic contribution of $\Delta T_{rms} = 4\mu\text{K}$ in the results at 33 GHz. An improved separation between the Galactic and the cosmological signal at each frequency will be presented in a forthcoming paper. We have removed the effects of the Sun and Moon to better than 50 dB in each daily scan, and stacking n days of observations with the Sun and Moon in different positions will reduce any residual contribution to an insignificant level.

The thermal noise contribution from the receivers conforms to a random Gaussian distribution and integrates down accordingly. In each instrument, the channel 1 receiver is fully independent of the channel 2 receiver and hence there is no correlation between the receiver noise in the data recorded for the two channels. Atmospheric emission varies randomly over days and thus at each frequency, stacking together n days of observations reduces the atmospheric signals in a given day by \sqrt{n} . Additionally, the Tenerife observing strategy is such that the *independent* 10, 15 and 33 GHz instruments observe *different* declination strips on any given day so that the atmospheric contribution to data taken at each frequency is uncorrelated. This offers a key advantage over experiments such as Saskatoon (Wollack *et al.* 1993), where the data in all of the frequency channels are highly correlated thus introducing an element of uncertainty due to the need to account for this. In our individual measurements the atmospheric contribution to each channel is correlated, since the timescale of the receiver switching is short compared with that for typical atmospheric fluctuations. In previous papers (Davies *et al.* 1987, Watson *et al.* 1992, Hancock *et al.* 1994 and Gutiérrez *et al.* 1995) this effect was not considered. The presence of a correlated atmospheric component affects the estimation of the astronomical signal based on the difference of the $(A+B)/2$ and $(A-B)/2$ data sets (A and B being separate subsets of the data). In particular if A and B each correspond to one channel, $(A+B)/2$ contains the contribution of the astronomical signal, and the atmospheric and instrumental noise, whilst $(A-B)/2$ only contains the instrumental noise. This is the case for the analysis of the 33 GHz data presented in Hancock *et al.* (1994) and therefore the signal level obtained from the difference in variance between the $(A+B)/2$ and $(A-B)/2$ scans contains a contribution from the atmosphere as well as the astronomy. Note that at 15 GHz the data were subdivided according to the observing epoch and consequently the contribution of the atmosphere to the derived signal was largely reduced.

Here we present a new split of the 33 GHz data into two subsets X and Y such that both channels of a given scan are included in the same data subset. Considering the non-repeatability of the atmosphere from day to day common atmospheric signals are not expected to occur in both

subsets. Also, considering the large number of independent observations (more than 50 for each channel) we expect that the net effect of the atmospheric signals will be just an increase of the variance in the final stacked scans of each subset, this increase in variance being approximately the same in both. For these reasons, when X and Y are combined to form the $(X+Y)/2$ and the $(X-Y)/2$ scans we expect to have approximately the same atmospheric signals in the sum and in the difference. Figure 2 shows the stacked data scans for the X and Y subsets and their sum and difference. We see a general agreement between the results of splits X and Y , and the presence of common features in both. An analysis similar to that presented in Hancock *et al.* (1994) gives an astronomical signal ($\sigma_s^2 = \sigma_{(X+Y)/2}^2 - \sigma_{(X-Y)/2}^2$) with an amplitude $\sigma_s = 43 \pm 12 \mu\text{K}$. The value of the signal quoted in Hancock *et al.* was $\sigma_{old} = 49 \pm 10 \mu\text{K}$; the difference with our improved estimation is certainly due to the subtraction of the atmospheric signal. The difference between both estimates ($\sigma = (\sigma_{old}^2 - \sigma_s^2)^{1/2}$) is $\sim 23 \mu\text{K}$ which is our best assessment of the atmospheric contamination in the analysis based on the addition and difference of the 33 GHz data; this value is in good agreement with estimates obtained using other methods.

3 STATISTICAL ANALYSIS

The estimates of the astronomical signals made in the previous section can be improved on using a detailed statistical analysis. Here we use a likelihood analysis and take into account the contribution of the correlated atmospheric noise by enlarging the error bars on the scans as shown in Figure 1. These modified scans are also used to study the presence of common features at 15 and 33 GHz by the calculation of the cross-correlation function.

3.1 Likelihood analysis

This analysis takes into account all the relevant parameters of the observations: experimental configuration, sampling, binning, etc. The combination of the atmospheric and instrumental noise can be modeled by a Gaussian distribution uncorrelated from point to point, (see previous section), which implies that the noise only contributes to the diagonal terms of the covariance matrix. We also assume that the astronomical signal is described by a Gaussian random field and therefore our results correspond to a superposition of Gaussian fields in which all their statistical properties are specified by the covariance matrix, which takes into account the full correlation between the data points.

We have analyzed our results for two hypothetical sky models, the first of which corresponds to a signal described by a Gaussian auto-correlation function (ACF) with amplitude $\sqrt{C_0}$ and width θ_c . This is not a realistic physical scenario but has been used widely in the past (Davies *et al.* 1987, Readhead *et al.* 1989, Watson *et al.* 1992) because it provides for an easy comparison between the results of experiments with different configurations. The intrinsic ACF for these models is given by

$$C(\theta) = C_0 \exp\left(-\frac{\theta^2}{2\theta_c^2}\right). \quad (1)$$

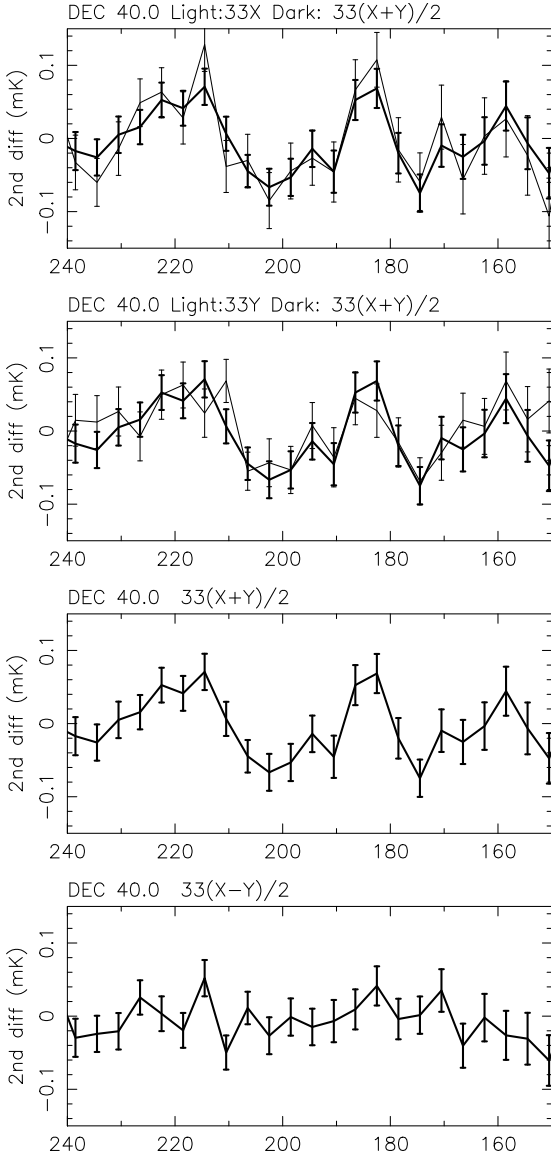


Figure 2. The data scans obtained from the analysis of two subsets of the 33 GHz data. In a) and b) are shown the subsets denoted X and Y which are constructed such that the atmospheric contributions to each are independent: see main text for details. The differences in the $(X+Y)/2$ (panel c)) and $(X-Y)/2$ (panel d)) scans should therefore be due only to astronomical signals.

which is modified accordingly by our triple beam filtering (Watson *et al.* 1992). Our instrument is sensitive over a range of coherence angles $1^\circ \lesssim \theta_c \lesssim 10^\circ$, attaining peak sensitivity for a coherence angle of 4° . We have analyzed the X and Y subsets for 15 and 33 GHz, the total stacked scans at these two frequencies, and our best scan 15+33. The results for $\theta_c = 4^\circ$ are presented in the third column of Table 1. The amplitude of the intrinsic signal corresponding to the maximum likelihood is given, along with the one-sigma confidence bounds calculated in a Bayesian sense with uniform prior. All results look consistent with clear detections at the two to three sigma level, and mean values of the signal slightly smaller than those presented in Hancock *et al.*, due to our improved estimate of the error bars in the stacked

scans (see Section 2 and Paper I). Figure 3 presents the contours of equal probability for the 15+33 scan. We see a well defined point of maximum likelihood at $\theta_c \sim 4^\circ$ and $\sqrt{C_0} \sim 50 \mu\text{K}$.

The second model considered here is more interesting from a cosmological viewpoint. It corresponds to the prediction of the power law form ($P(k) \propto k^n$) for the spectrum of the primordial fluctuations. Considering only the Sachs-Wolfe part of the spectrum of the fluctuations the intrinsic ACF can be expressed as

$$C(\theta) = \frac{Q_{rms-ps}^2}{5} \sum_l (2l+1) C_l^{(S)} P_l(\cos\theta) \quad (2)$$

$$C_l^{(S)} = C_2^{(S)} \frac{\Gamma[l + (n-1)/2] \Gamma[(9-n)/2]}{\Gamma[l + (5-n)/2] \Gamma[(3+n)/2]}$$

where the sum is extended to the multipoles $l \lesssim 60$ which corresponds to the range of angular sensitivity of our experiments. For $l \gtrsim 20$, standard models predict additional contributions to the CMB anisotropy, as one moves into the low l tail of the CMB Doppler peak. Hence fitting for the Sachs-Wolfe term alone (Equation 2) to CMB data on these scales can lead to the derived values for n being increased by as much as 10% over the true primordial value. This point should be borne in mind when comparing the limits on n from the Sachs-Wolfe term (Sections 3 and 4) to those from a fit to a full CDM type functional form as in Section 5.

For a given value of the spectral index n , the intrinsic ACF is a function only of Q_{rms-ps} . Figure 4 shows the likelihood surface as a function of Q_{rms-ps} and n for the 15+33 scan. The peak likelihood forms a ridge displaced from zero in Q_{rms-ps} and corresponds to a 3–4 sigma detection of structure for each value of n considered. The shape of the surface implies that all values of n in this range are equally likely. This is predominantly a consequence of our observing technique which samples only a small angular range of the spectrum of fluctuations. Thus whilst our observations provide a good measure of the fluctuation power on $\sim 4^\circ$ scales, they do not in themselves contain sufficient information about the distribution of power with angular scale to allow a useful determination of the spectral slope: for this one must compare with experiments on other angular scales (see Sections 4 and 5). For the specific case of a Harrison-Zel'dovich spectrum ($n = 1$) the results of the likelihood analysis are given in column two of Table 1. The normalisation Q_{rms-ps} corresponds to the maximum of the likelihood function and the confidence intervals are at 68 %, calculated in the standard Bayesian manner using uniform prior. We see that in general the results are consistent and agree with a global normalization of the quadrupole $Q_{rms-ps} \sim 20 - 25 \mu\text{K}$. Our best estimate for Q_{rms-ps} of $22_{-6}^{+10} \mu\text{K}$ from the 15+33 scan is reduced over the value of $26 \pm 6 \mu\text{K}$ previously reported due to our now having properly accounted for the correlated atmospheric noise.

3.2 Cross-correlation analysis

We have investigated the presence of common features in our 15 + 33 scans at Dec=+40° by evaluating the cross-correlation function,

Table 1. Results of the likelihood analysis for a Harrison-Zel'dovich spectrum of fluctuations (second column) and for a Gaussian ACF (third column).

ν (GHz)	Q_{rms-ps} (μK)	$\sqrt{C_0}$ (μK)
15A	27^{+16}_{-16}	54^{+37}_{-30}
15B	17^{+9}_{-17}	24^{+21}_{-24}
15	21^{+12}_{-9}	44^{+26}_{-19}
33A	22^{+14}_{-10}	45^{+32}_{-24}
33B	28^{+12}_{-9}	57^{+28}_{-25}
33	24^{+11}_{-8}	49^{+27}_{-17}
15+33	22^{+10}_{-6}	48^{+21}_{-15}

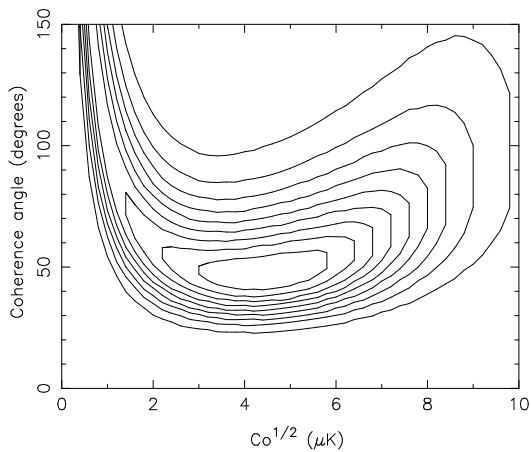


Figure 3. Contour levels of equal likelihood for the 15+33 scan in the case of a Gaussian shaped ACF. The contours correspond to 10, 20, 30 ... 90 % of the total probability distribution. The Tenerife configuration obtains maximum sensitivity for coherence angles in the range $2^\circ \lesssim \theta \lesssim 6^\circ$; structure is clearly detected at $\sim 50\mu\text{K}$ over this angular scale range.

$$C(\theta) = \frac{\sum_{i,j} \Delta T_i \Delta T'_j w_i w'_j}{\sum_{i,j} w_i w'_j} \quad (3)$$

where ΔT and $\Delta T'$ denote the second differences in the stacked scans at 15 and 33 GHz respectively. The sum is extended over all points subtending a mutual angle θ in RA, with weights $w_i = 1/\sigma_i^2$ and $w'_j = 1/\sigma'_j{}^2$ respectively. The

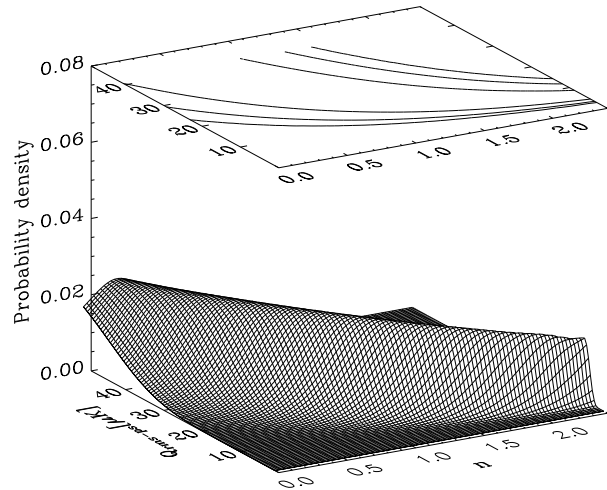


Figure 4. The two-dimensional normalised likelihood surface as a function of the spectral index n and the normalisation Q_{rms-ps} for the Tenerife data. The projected contours are at 68 %, 95 % and 99 % confidence.

data points in Figure 5 represent the mean and 68 % confidence intervals of $C(\theta)$. The observed profile is characteristic of the triple beam sampling and it is clear that for angles $\theta \lesssim 20^\circ$ the results are consistent with the presence of common signals in the two independent data sets. Because of the non-independence of the data points in the cross-correlation function, the statistical significance is difficult to evaluate, requiring the computation of the covariance matrix of the correlation function (see *e.g.* Ganga *et al.* 1993). However, considering only the correlation at zero lag, the observed value of $C(\theta) = 1100^{+680}_{-720} \mu\text{K}^2$ is found to be inconsistent with noise at the 95 % level. This value for the amplitude of the component of the signal common to the 15 and 33 GHz data is in agreement with the equivalent estimates of the variance of the signals present in each data scan separately, demonstrating that common signals can account for all of the structure seen in the separate scans. This is contrary to what one expects for structure of Galactic origin, which in the case of synchrotron and free-free emission would exhibit a change in amplitude by a factor 9 and 5 respectively on moving from 15 GHz to the higher frequency of 33 GHz. This result taken in conjunction with the limits on the Galactic contamination of the 33 GHz scan (see above) and the successful comparison of the features seen in the 15 and 33 GHz scans with the higher frequency COBE data (Lineweaver *et al.*, 1995), leads us to assign a cosmological origin to the majority of the signal present in the 15 GHz data.

We have explicitly tested the consistency of the common signals with fluctuations originating in inflationary type models which predict an approximately scale invariant $n \simeq 1$ spectrum of fluctuations. Using the normalisation of $Q_{rms-ps} = 22\mu\text{K}$ as derived from the likelihood analysis of the 15+33 scan we simulated 5000 realisations of a sky conforming to a Harrison-Zel'dovich spectrum and repeated the Tenerife sampling strategy. The mean value (solid line) and one-sigma confidence intervals (dashed lines) of

the auto-correlation function obtained from these realisations are plotted in Figure 5. There is clearly a good level of agreement in the amplitude and shape of the experimental results and the theoretical model. Statistically the Tenerife observations have the properties expected for primordial fluctuations generated from inflation, and although these results do not prove inflationary theory, this does offer a plausible explanation for the existence of structure on scales greater than the horizon volume at recombination. In this case, the clearly defined structures visible in the scans in Figure 1 represent the seed perturbations generated in the inflationary era at $t < 10^{-34}$ s. In the following section we investigate the potential to prove or disprove inflation by measuring the slope n of this primordial spectrum of fluctuations using large scale CMB anisotropy measurements.

4 STATISTICAL COMPARISON WITH COBE DMR

A comparison between the results of different CMB experiments offers the opportunity to check independent measurements, to extend the range in frequency and angular scale, to constrain cosmological models and, if the sensitivity of the experiments is sufficient, to compare features. There are several experiments operating on angular scales of a few degrees: MIT (Ganga *et al.* 1993), COBE (Smoot *et al.* 1992, Bennett *et al.* 1994), RELIKT (Strukov *et al.* 1993), ARGO (De Bernardis *et al.* 1994a) and Tenerife. The first comparison between independent CMB observations was made by Ganga *et al.* (1993) who found a clear correlation between the results of the first year of COBE DMR observations and those of the MIT experiment. De Bernardis *et al.* (1994b) have also made a statistical comparison between the amplitude of the signal reported for ARGO and that of the COBE DMR first year results, from which they constrain the spectral index to be $0.5 \leq n \leq 1.2$ in the absence of any gravity wave background. In our preliminary report (Hancock *et al.* 1994) we compared the amplitude of the signal detected on $\sim 5^\circ$ scales in our Dec= $+40^\circ$ data with that on $\sim 7^\circ$ scales for the first year of COBE data. We found that both results were consistent with inflationary models ($n \gtrsim 0.9$) but with a favoured spectral index of $n = 1.6$. Lineweaver *et al.* (1995) have presented the first direct comparison of CMB features between the two-year COBE DMR data and the Tenerife Dec= $+40^\circ$ observations, confirming the agreement in the level of the normalization of both experiments and providing clear evidence for the presence of common hot and cold spots in both data sets. The comparison presented here is different to that conducted in Hancock *et al.* (1994) in that we use a more rigorous comparison technique that utilises the likelihood function to incorporate fully the effects of cosmic and sample variance, random noise and the interdependence of the model parameters. In addition to the improvements from this revised analysis, our new results also reflect the increased sensitivity of the COBE data after two years of observing, along with the more accurate estimate of the cosmological signal in the Tenerife data.

4.1 Properties of the two data sets

The instrumental profile of the COBE data is described approximately by a Gaussian beam with $\text{FWHM} \sim 7^\circ$. As can be seen in Figure 1 of Watson *et al.* (1992) there is a range of angular scales to which the COBE DMR and Tenerife experiments are both sensitive. Measurements taken by COBE cover the full sky, but to determine the CMB fluctuations the region of the Galactic plane has been excluded ($|b| \leq 20^\circ$) thereby introducing a degree of uncertainty in estimating the properties of the global field; this effect is commonly termed sample variance (Scott, Srednicki & White 1994). The uncertainties in the COBE two year results are dominated by the effect of cosmic variance *i.e.* the fact that our stochastic theory describes the Universe as a particular realisation of a random field. Together the cosmic and sample uncertainties form an intrinsic limitation of the COBE experiment since unlike random errors they are not reduced by increased integration time. The two year COBE data have been analysed independently by a number of authors (*e.g.* Banday *et al.* 1994, Bennett *et al.* 1994, Bond 1994, Gorski *et al.* 1994, Wright *et al.* 1994). All find evidence for statistically significant structure at an amplitude consistent with that of $30 \pm 5 \mu\text{K rms}$ on a 10° scale announced by Smoot *et al.* (1992) for the first year data. The best fit values for n and Q_{rms-ps} depend on the precise analysis techniques employed, but are generally consistent with the values of $n = 1.10 \pm 0.29$, $Q_{rms-ps} = 20.3 \pm 4.6 \mu\text{K}$ found by Tegmark and Bunn (1995) for the combined 53 and 90 GHz data with the quadrupole included. In the case of the Tenerife experiment the double-switching scheme removes the contribution of low order multipoles decreasing the cosmic variance of the signal on these large scales; the major source of uncertainty is produced by the partial sky coverage (sample variance) and the instrumental noise. The region observed by the Tenerife experiments covers ~ 5000 square degrees but here we have limited our analysis to our region of deepest integration at high Galactic latitude which constitutes a sample ~ 500 square degrees. For such a region the uncertainties due to the partial sky coverage dominate over the intrinsic variance by a factor ~ 10 (Scott, Srednicki & White 1994) and the combined uncertainty is approximately of the order of that introduced by the instrumental noise in the 15+33 scan.

In previous work (Hancock *et al.* 1994) we explicitly took into account the effects of cosmic and sample variance by using Monte Carlo simulations. This was necessary because the simple excess variance statistic used in the comparison incorporated only the uncertainty due to random noise. The comparison by necessity assigned equal probability to all values of n for the COBE data, since the COBE first year results were only published in the form of a best fit n versus Q_{rms-ps} relation rather than a full two dimensional probability distribution. What is required is a data analysis technique that allows the joint probability of any combination of the model parameters to be calculated and which implicitly takes into account random errors and cosmic and sample uncertainties. The Bayesian approach using the likelihood function as described in Section 3 attempts to do precisely this. The likelihood function peaks at the most likely parameters (the best estimate of the true values if the likelihood function is unbiased) and has some distri-

bution which through Bayes theorem is representative of the combined effects of the cosmic, sample and random uncertainties. The issue of how well this distribution reflects the true uncertainties is addressed explicitly in a forthcoming paper (Rocha *et al.* in preparation) by comparison of the Bayesian probability distribution with that obtained from direct Monte Carlo simulations of the data. The Bayesian and frequentist approaches are found to be consistent for the Tenerife data and to a good approximation the likelihood function is also seen to be an unbiased estimator of the model parameters. Consequently the likelihood surface for the joint Tenerife and COBE data set provides the definitive means of comparison of the observations under some assumed sky model.

4.2 The Tenerife-COBE likelihood function

Here we apply the likelihood analysis to the COBE two year data and the Tenerife 15+33 scan, assuming a power law model with free parameters n and Q_{rms-ps} . The COBE Galaxy-cut two-year map consists of 4038 pixels, whilst the Tenerife Galaxy cut (RA $161^\circ - 230^\circ$) scan contains 70 pixels, requiring a 4108×4108 covariance matrix for a joint likelihood analysis of the data. The direct inversion of such a large matrix, necessary for the likelihood analysis, is computationally intensive, but has been implemented for the combined 53 and 90 GHz COBE two-year data by Tegmark and Bunn (1995), hereafter ‘‘TB95’’. A number of other authors (Bond 1994, Bunn and Sugiyama 1994, Gorski 1994) have computed the likelihood function by using various data compression techniques to reduce the size of the covariance matrix. The compression is achieved by discarding noisy data vectors whilst retaining most of the cosmological signal, and although the results are close to optimal, the slight loss of signal results in marginally larger error bars than the ‘‘brute force’’ approach. The latter method is conceptually the simplest one, since it is merely a likelihood analysis using all available data, and involves no adjustable parameters such as the degree of data compression. Since each matrix inversion requires merely about 10 minutes on a fast workstation, we use the brute force method here.

We arrange the pixels in a 4108-dimensional vector and compute the likelihood function as in TB95 by Cholesky decomposition of the 4108×4108 covariance matrix at a dense grid of points in the (n, Q_{rms-ps}) -parameter space, marginalizing over the four ‘‘nuisance parameters’’ that describe the monopole and dipole. The covariance matrix consists of three parts: a 70×70 block with the covariance between the Tenerife pixels, a 4038×4038 block with the covariance between the COBE pixels, and off-diagonal 4038×70 blocks containing the covariance between the Tenerife and COBE pixels. Simply multiplying the likelihood curves resulting from two separate analyses of the COBE and Tenerife data sets would correspond to neglecting the off-diagonal blocks, and this is clearly only a good approximation if the two data sets are almost uncorrelated. We find that the inclusion of the cross-terms makes a non-negligible difference, which is not surprising in view of the fact that the two experiments probe comparable angular scales and have observed a common region of the sky.

For our Tenerife data, the best estimate of the cosmological signal is obtained from the 15+33 combined scan

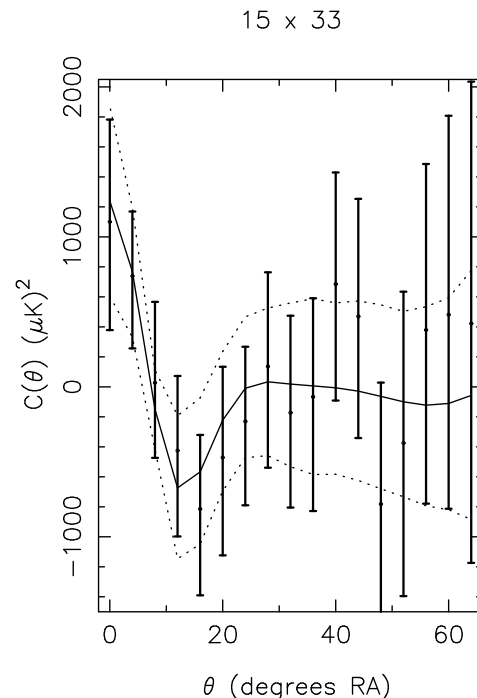


Figure 5. The cross-correlation function $C(\theta)$ for the 15 GHz and 33 GHz data over RA= $161^\circ - 230^\circ$ showing the data points and the one sigma error-bars. The solid line corresponds to the prediction of a Harrison-Zel'dovich spectrum of fluctuations with a normalization of $Q_{rms-ps} = 22 \mu\text{K}$. The dashed lines are the 1σ confidence bounds arising from cosmic variance and sample variance.

after correction of the error bars for the correlated atmospheric noise term. The possible contribution of Galactic signals has been estimated from the 10 GHz data to be less than $4 \mu\text{K}$ at 33 GHz and has not been considered in the current comparison. The normalised likelihood function for this scan, as plotted in Figure 6, represents the joint probability of obtaining a given combination of n and Q_{rms-ps} . On its own, the Tenerife configuration provides less leverage on the slope of the spectrum than the COBE satellite. This is because the Tenerife experiment is insensitive to the largest angular scales, and because the one-dimensional shape of the dec+ 40° strip makes it difficult to separate the power contributions from different scales. In other words, a narrow strip corresponds to wide window functions in ℓ -space, with considerable aliasing of small-scale power onto larger scales (just as the case is with one-dimensional ‘‘pencil beam’’ galaxy surveys). As a result, the Tenerife data can be equally well fit by a range of n and Q_{rms-ps} values, resulting in a likelihood ridge in (n, Q_{rms-ps}) -space with minimal discriminatory power for the parameter n . In contrast, the COBE observations are sensitive to the slope to the extent that the likelihood surface is peaked in the n -dimension. Combining the COBE information with the Tenerife data improves the situation in two ways: it extends the lever arm on the spectral slope from the COBE scales down to the 4° scale of Tenerife, and in addition eliminates the above-mentioned aliasing problem, since the joint data set is no longer one-dimensional.

Figure 6 shows the confidence contours obtained from

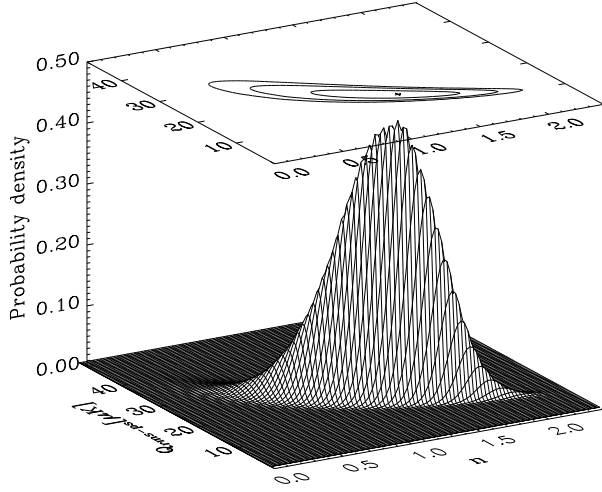


Figure 6. Constraints on the quadrupole Q_{rms-ps} and on the spectral index n of fluctuations obtained from a joint likelihood analysis of the Tenerife data and COBE DMR two-year data. The contour levels represent 68 %, 95 % and 99 % of the region of joint probability. The peak of the distribution lies at $n = 1.37$, $Q_{rms-ps} = 16.1\mu\text{K}$ and is identified by the cross.

Bayesian integration under the combined COBE and Tenerife likelihood surface assuming a uniform prior. The 68% joint confidence region in (n, Q_{rms-ps}) -space encloses a region from 0.90 to 1.73 in n for Q_{rms-ps} in the range from 12.1 to 22.9 μK , with the peak at $n = 1.37$, $Q_{rms-ps} = 16.1\mu\text{K}$. Marginalizing over Q_{rms-ps} with a uniform prior, one obtains the probability distribution for n as given in Figure 7, corresponding to $n = 1.33 \pm 0.30$ at 68% confidence. The resulting limits on the normalization, conditioned on $n = 1$ as is customary, are $Q_{rms-ps} = 21.0 \pm 1.6$. The corresponding results in TB95 using just the COBE data, and including the weak correlated noise term (Lineweaver *et al.* 1995), were $n = 1.10 \pm 0.29$ and $Q_{rms-ps} = 20.3 \pm 1.5$, with the peak likelihood located at $n = 1.15$, $Q_{rms-ps} = 18.2\mu\text{K}$. In other words, although the total normalization has risen by a mere 3%, the slope estimate has risen by 12% and the peak likelihood has been shifted to higher n and lower Q_{rms-ps} . This indicates that the higher angular resolution data from the Tenerife experiment contains slightly more power on small scales. As explained in Section 3.1, this is not unexpected, since the presence of a Doppler peak would cause a rise in the power spectrum at higher l .

5 ADDITIONAL CONSTRAINTS ON THE PRIMORDIAL SPECTRAL INDEX

The large angular scale CMB observations from Tenerife and COBE probe fluctuations that have yet to go non-linear and the shape of the power spectrum is thus insensitive to the exact abundance of the baryonic mass (Ω_b) and to the value of $h = H_0/100 \text{ km s}^{-1} \text{ Mpc}^{-1}$. However, together the Tenerife and COBE observations provide a direct measure of the CMB power spectrum normalisation, against which one can compare intermediate scale observations and hence discriminate between competing cosmological models. Here

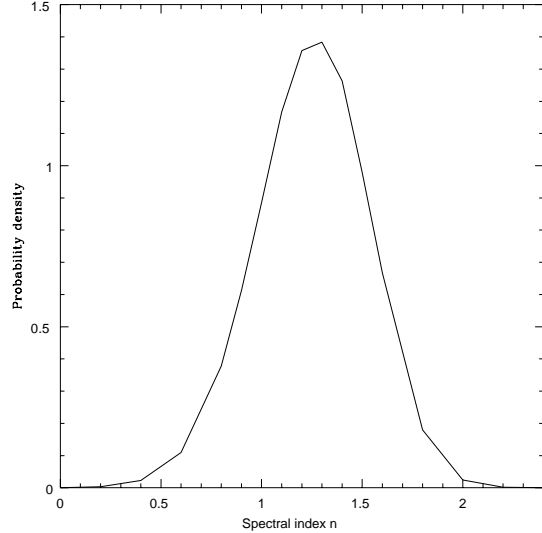


Figure 7. The marginal likelihood for the spectral index n as obtained from the joint analysis of the Tenerife and COBE data. The spectral index is seen to lie in the range $1.02 \leq n \leq 1.62$ at 68% confidence, with a best fit value of $n = 1.33$.

we stress the importance in the agreement between the derived normalisation for the independent Tenerife and COBE experiments, which are subject to different systematic errors and different foreground contamination. The accuracy to which we know the normalisation of the power spectrum clearly becomes an issue when comparing with smaller scale observations to determine cosmological parameters. This is a particular concern if, as has been suggested (Crittenden *et al.* 1993, Steinhardt 1993, Abbott and Wise 1984), a component of the large scale anisotropy may be due to tensor metric perturbations produced from a background of gravitational waves. These can arise naturally in inflationary scenarios and would contribute a component $C_l^{(T)} = \langle |a_{lm}^T|^2 \rangle$ to the observed CMB angular power spectrum (cf Equation 2). The ratio of the tensor modes $C_l^{(T)}$ to the scalar modes $C_l^{(S)}$ (primordial density fluctuations) is highly suppressed for fluctuations contained within the horizon volume at recombination and hence their contribution is only significant on scales $\gtrsim 2^\circ$. Consequently the existence of a tensor contribution has implications when comparing the large scale anisotropy level with that on smaller scales and with large scale structure observations in order to test cosmological models. The anisotropy measurements from Tenerife and COBE fix the sum of $C_l^{(T)}$ and $C_l^{(S)}$, but the separation of the two terms requires a comparison with smaller scale observations under the assumption that a given cosmological model is correct (Crittenden *et al.* 1993, Steinhardt 1993). In the case of power law inflation a relation exists between the tensor to scalar ratio $C_2^{(T)}/C_2^{(S)}$ and the slope of the primordial power spectrum (Crittenden *et al.* 1993, Steinhardt 1993) :

$$C_2^{(T)}/C_2^{(S)} \approx 7(1 - n) \quad (4)$$

from which we see that the two contributions are comparable at $n = 0.85$ with $C_l^{(T)}$ decreasing relative to $C_l^{(S)}$ for higher values of n . Thus the limit of $n \geq 1.0$ obtained from the

analysis of the combined Tenerife and COBE data in Section 4.2 implies that it is unlikely that the tensor component will be dominant in such models. In the remainder of this section we shall investigate this in more detail by comparing with medium-scale anisotropy results.

Contemporary cosmological models with adiabatic fluctuations predict a sequence of peaks on the power spectrum which are generated by acoustic oscillations of the photon-baryon fluid at recombination. Of particular interest is the height and position of the main acoustic peak — the so called Doppler peak: the height depends on quantities like the baryonic content of the universe, Ω_b , and Hubble constant, H_0 , whilst the position depends on the total density of the Universe, Ω_0 .

The work required to place the existing medium scale anisotropy results into a common statistical framework and then to compare them with the predictions of cosmological models, has been carried out by Hancock *et al.* (submitted) who find strong evidence for the existence of a Doppler peak on medium scales. Further details together with a comparison with a fuller range of cosmological models will be presented in Rocha *et al.* (in preparation). For the current purpose of discussion of the value of n , and comparison with the results obtained from Tenerife and COBE alone, we present here a version of the results for n found in Hancock *et al.* (submitted).

The precise form of the Doppler peak depends on the nature of the dark matter, and the values of Ω_0 , Ω_b and H_0 . Thus in order to use the medium-scale anisotropy results to provide additional leverage on the spectral index determination it is necessary to adopt a given cosmological model. Taking the minimalist assumption of the standard Cold Dark Matter (CDM) model, without gravity waves, with $H_0 = 50 \text{ km s}^{-1} \text{ Mpc}^{-1}$, $\Omega_b = 0.07$, Hancock *et al.* (submitted) find this offers a good fit to all of the data. Tilting the initial spectrum of fluctuations away from scale invariance and fitting to the ΔT_l we can delimit n using the full data set.

Hancock *et al.* considered the four-year COBE data, and used the binned angular power spectrum (Tegmark 1996) in conjunction with Tenerife, Python, South-Pole, Saskatoon, MAX, ARGO, MSAM and CAT experiments. As seen in Figure 8, only models with initial spectra in the range $1.0 \leq n \leq 1.2$ are allowed by this improved analysis, with best fit values of $Q_{rms-ps} = 15 \mu\text{K}$ for $n = 1.1$. These results are consistent with those from large scales alone, and with the inflationary value of $n \simeq 1.0$. We note that the presence of a gravity wave component in our model would require even larger values of n than those derived above and given Equation 4 this reaffirms our conclusion that a significant gravity wave contribution is unlikely. The above constraint on n depends on which values of Ω_0 , Ω_b and H_0 are chosen, but is not simply related to any one parameter. Constraints on n derived using a fuller set of models are given in Rocha *et al.* (in preparation).

Prior to the COBE detection the most common normalization of models used was based on the value of σ_8 ($(\Delta M/M)_{rms}$ in a sphere of radius $8h^{-1} \text{ Mpc}$) derived from galaxy clustering assuming a bias $b = 1$ *i.e.* that light traces mass (Kaiser 1984, Davis *et al.* 1985). If in fact galaxies are more highly clustered than matter, the amplitude of the initial matter perturbations (and hence $\Delta T_{rms}/T$) necessary

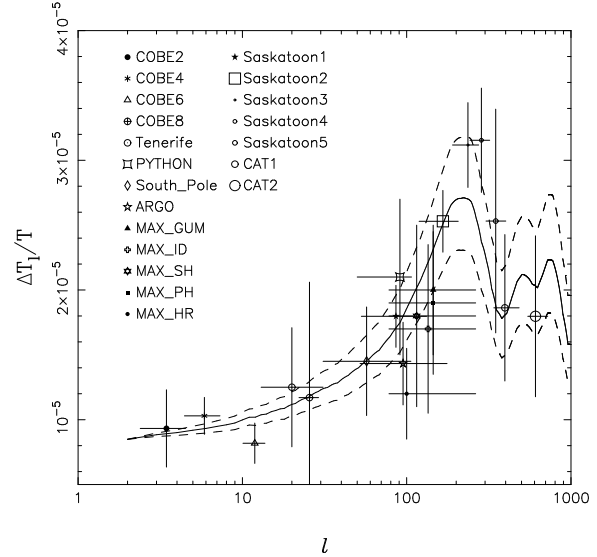


Figure 8. Recent CMB anisotropy results on large and intermediate angular scales are used to delimit the spectral index n of the primordial fluctuations.

to produce the observed clustering is reduced by the factor b . The Tenerife and COBE data provide an independent and more accurate value for the normalisation which for a given cosmological model allows us to determine the degree of bias necessary for consistency with the large scale structure observations.

In particular the COBE normalized CDM model with a tilt of $n = 1.1$ gives a bias of the order $\simeq 0.7$.

6 DISCUSSION AND CONCLUSIONS

We have presented a detailed analysis of the measurements taken at Dec= $+40^\circ$ by the Tenerife experiments at 10, 15 and 33 GHz. After accounting for both local atmospheric and discrete radio source foregrounds, the 15 and 33 GHz data at high Galactic latitude are seen to contain statistically significant signals which have their origin in common hot and cold features. The cross-correlation function between the data at these two frequencies demonstrates that the amplitudes and shapes of the structures detected at 15 and 33 GHz are similar. This, combined with our measurements at the lower frequency of 10 GHz, implies that the CMB signal dominates over the Galactic contribution at 15 GHz, and that the maximum possible Galactic contribution at 33 GHz is smaller than 10 % of the detected signal. Our best estimate of the cosmological signal is $Q_{rms-ps} = 22_{-6}^{+10} \mu\text{K}$ for an $n = 1$ inflationary spectrum. This amplitude is reduced by $4 \mu\text{K}$ over that previously reported for the same data set and results from an improved separation of signal from atmospheric noise. Comparison of the Tenerife and COBE two year anisotropy detections by means of the likelihood function allows a detailed investigation of the allowed parameter space for a power law model of the fluctuation spectrum. The best fit values of n and Q_{rms-ps} are 1.37 and $16 \mu\text{K}$, and marginalising over Q_{rms-ps} we find both data sets consistent with n in the range $1.0 \leq n \leq 1.6$. These results support inflationary

models, which predict $n \simeq 1$ and future improvements in the Tenerife data and use of the 4 year COBE data will narrow the range of allowed n . Improvements of this kind are important to determine the power spectrum normalisation, since *only* on these large angular scales is it possible to place limits on the tensor to scalar ratio independent of the precise details of the cosmological model. By combining the large scale anisotropy measurements from Tenerife and COBE with observations of medium scale anisotropy measurements, improved limits have been placed on n , but at the expense of assuming an underlying cosmological model (in our case CDM).

For a CDM model with $H_0 = 50 \text{ km s}^{-1} \text{ Mpc}^{-1}$, $\Omega_b = 0.07$, we find that this data set is consistent with n in the range $1.0 \leq n \leq 1.2$. The best fit values of n and Q_{rms-ps} are 1.1 and $15 \mu\text{K}$. This COBE normalized tilted model predicts a bias of the order $\simeq 0.7$. So although this model fits well the CMB data alone it may not give a realistic scenario when we consider jointly the CMB data and the observed galaxy clustering.

Our attempts to place increasingly more accurate limits on fundamental cosmological parameters will undoubtedly place increasing demands on observers for ever improved accuracy until the point where the intrinsic cosmic variance becomes the dominant form of error. Confidence in the results to this tolerance level will probably require close co-operation between observers and the combination of results from space-based, balloon-based and ground-based telescopes working over a range of frequencies. Potentially the most powerful observations will result from mapping overlapping/ interlocking CMB fields with independent multi-frequency instruments. In contrast to the statistical results currently being reported, this method builds in the necessary redundancy to reduce systematic errors to an acceptable level. Such observations are currently in progress with the Tenerife instruments, which in conjunction with the COBE 4 year data should provide a high signal to noise map of the last scattering surface thus providing a two dimensional representation of the seed structures as compared to the simple 1-D scans reported here. Being on scales greater than the horizon size at recombination the form of such a map would reflect the structures generated in an inflationary driven phase in the very early universe.

ACKNOWLEDGMENTS

The Tenerife experiments are supported by the UK Particle Physics and Astronomy Research Council, the European Community Science programme contract SCI-ST920830, the Human Capital and Mobility contract CHRXCT920079 and the Spanish DGICYT science programme. S. Hancock wishes to acknowledge a Research Fellowship at St. John's College, Cambridge. G. Rocha wishes to acknowledge a JNICT studentship from Portugal.

REFERENCES

Abbott, L.F. & Wise, M. 1984, Nucl. Phys. B244, 541
 Aizu, K., Inoue, M., Tabara, H., & Kato, T. 1987, 124th IAU symp. "Observational Cosmology", 565, Reidel Publishing Company

Banday, A.J. *et al.* 1994 ApJ, 436, L99
 Bardeen, J.M., Steinhardt, P.J. & Turner, M.S., 1983, Phys. Rev. D., 28, 679
 Bennett, C.L. *et al.* 1994, ApJ, 436, 423
 Bond, J.R., 1994, Phys. Rev. Lett., 74, 4369
 Bond, J.R. & Efstathiou, G. 1987, MNRAS, 226, 655
 Bunn, E.F. and Sugiyama, N. 1995, ApJ, 446, 49
 Cheng, E.S., *et al.* 1996, ApJ, 456, L71
 Clapp, A. *et al.* 1994, ApJ, 433, L57
 Crittenden, R., Bond, J.R., Davis, R.L., Efstathiou, G. and Steinhardt, P.J. 1993, Phys. Rev. Lett., 71, 324
 Davis, M., Efstathiou, G., Frenck, C.S. & White, S.D.M. 1985, ApJ, 292, 371
 Davies, R.D., Watson, R.A., Daintree, E.J., Hopkins, J., Lasenby, A.N., 1987, Nature, 326, 462
 Davies, R.D., Watson, R.A., Daintree, E.J., Hopkins, J., Lasenby, A.N., Sanchez-Almeida, J., Beckmann, J.E., Rebolo, R., 1992, MNRAS, 258, 605
 Davies, R.D., *et al.* 1996, MNRAS, 278, 883 (Paper I)
 De Bernardis, P. *et al.* 1994a, ApJ, 422, L33
 De Bernardis, P., De Gasparis, G., Masi, S., & Vittorio, N. 1994b, ApJ, 433, L1
 Franceschini, A., Toffolatti, L., Danese, L., & De Zotti, G. 1989, ApJ, 344, 35
 Feldman, H., Kaiser, N. & Peacock, J. 1994, ApJ, 426, 23
 Ganga, K., Cheng, E., Meyer, S., & Page, L. 1993, ApJ, 410, L57
 Gorski, K.M. *et al.* 1994, ApJ, 430, L89
 Gundersen, J.O. *et al.* 1995, ApJ, 443, L57
 Gutierrez de la Cruz, C. M., Davies, R. D., Rebolo, R., Watson, R. A., Hancock, S. & Lasenby, A. N. 1995, ApJ, 442, 10
 Hancock, S., Davies, R.D., Lasenby, A.N., De La Cruz, C.M.G., Watson, R.A., Rebolo, R., Beckman, J.E., 1994, Nature, 367, 333
 Hancock, S., Rocha, G., Lasenby, A.N. & Gutierrez, C.M., 1997, MNRAS (submitted)
 Kühr, H., Witzel, A., Pauliny-Toth, I.I.K., & Nauber, U. 1981, A&AS, 45, 367
 Kaiser, N. 1984, ApJ, 284, L9
 Knox, L. and Turner, M. 1994, PRL, 73, 3347
 Lineveaver, C.H., Hancock, S., Smoot, G.F., Lasenby, A.N., Davies, R.D., Banday, A.J., De La Cruz, C.M.G., Watson, R.A., Rebolo, R., 1995, ApJ, 448, 482
 Maddox, S.J., Efstathiou, G., Sutherland, W.J., and Loveday, J. 1990, MNRAS, 242, 43
 O'Sullivan, C. *et al.* 1995, MNRAS, 274, 861
 Pagel, B.E.J. 1991 Phys. Scripta, T36, 7
 Readhead, A.C.S. *et al.* 1989 ApJ, 346, 566
 Robson, R. *et al.* 1993, A & A, 277, 314
 Schuster, J. *et al.* 1993, ApJ, 412, L47
 Scott, D., Srednicki, M., White, M., 1994, ApJLett, 421, L5
 Scott, D., Silk, J. and White, M., 1995, Science, 268, 829
 Smoot, G.F. *et al.* 1992, ApJ, 396, L1
 Steinhardt 1993, Proc. of the Yamada Conference XXXVII 'Evolution of the Universe and its Observational Quest', p159-180.
 Strukov, I.A., Brukhanov, A.A., Skulachev, D.P., & Sazhin, M.V. 1993, Phys. Lett., B, 315, 198
 Tegmark, M., Bunn, E.F., 1995, ApJ, 455, 1
 Tegmark, M., 1996, ApJ, 464, L35
 Watson, R.A., De La Cruz, C.M.G., Davies, R.D., Lasenby, A.N., Rebolo, R., Beckmann, J.E., Hancock, S., 1992, Nature, 357, 660
 White, M., Scott, D. & Silk, J., 1994, Ann. Rev. Astron. Astrophys., 32, 319
 Wollack, E.J., Jarosik, N.C., Netterfield, C.B., Page, L.A., & Wilkinson, D., 1993, ApJ, 419, L49
 Wright, E.L. *et al.* 1994, ApJ, 436, 452